metals

MDPI

Article

Characteristics of Microstructure Evolution during FAST Joining of the Tungsten Foil Laminate

Xiaoyue Tan [1,2,3,*], Wujie Wang [1], Xiang Chen [4], Yiran Mao [2,3], Andrey Litnovsky [2,5], Felix Klein [2], Pawel Bittner [2], Jan Willem Coenen [2,6], Christian Linsmeier [2], Jiaqin Liu [4], Laima Luo [1,7] and Yucheng Wu [1,7,8,*]

1 School of Materials Science and Engineering, Hefei University of Technology, Hefei 230009, China; wjwang92@126.com (W.W.); luolaima@126.com (L.L.)
2 Forschungszenturn Jülich GmbH, Institut für Energie- und Klimaforschung—Plasmaphysik, Partner of the Trilateral Euregio Cluster (TEC), 52425 Jülich, Germany; y.mao@fz-juelich.de (Y.M.); a.litnovsky@fz-juelich.de (A.L.); fe.klein@fz-juelich.de (F.K.); p.bittner@fz-juelich.de (P.B.); j.w.coenen@fz-juelich.de (J.W.C.); ch.linsmeier@fz-juelich.de (C.L.)
3 School of Mechanical Engineering, Hefei University of Technology, Hefei 230009, China
4 Institute of Industry & Equipment Technology, Hefei University of Technology, Hefei 230009, China; chenxiang2017@mail.hfut.edu.cn (X.C.); jqliu@hfut.edu.cn (J.L.)
5 Department of Plasma Physics, Institute of Plasma and Laser Technologies, National Nuclear Research University MEPhI, Kashirskoe sh.31, 115409 Moscow, Russia
6 Department of Engineering Physics, University of Wisconsin—Madison, Madison, WI 53706, USA
7 National-Local Joint Engineering Research Centre of Nonferrous Metals and Processing Technology, Hefei 230009, China
8 Key Laboratory of Interface Science and Engineering of New Materials, Ministry of Education, Taiyuan University of Technology, Taiyuan 030024, China
* Correspondence: xytan@hfut.edu.cn (X.T.); ycwu@hfut.edu.cn (Y.W.)

Citation: Tan, X.; Wang, W.; Chen, X.; Mao, Y.; Litnovsky, A.; Klein, F.; Bittner, P.; Coenen, J.W.; Linsmeier, C.; Liu, J.; et al. Characteristics of Microstructure Evolution during FAST Joining of the Tungsten Foil Laminate. *Metals* **2021**, *11*, 886. https://doi.org/10.3390/met11060886

Academic Editors: Milan Brandt and Andrey Belyakov

Received: 18 March 2021
Accepted: 26 May 2021
Published: 28 May 2021

Abstract: The tungsten (W) foil laminate is an advanced material concept developed as a solution for the low temperature brittleness of W. However, the deformed W foils inevitably undergo microstructure deterioration (crystallization) during the joining process at a high temperature. In this work, joining of the W foil laminate was carried out in a field-assisted sintering technology (FAST) apparatus. The joining temperature was optimized by varying the temperature from 600 to 1400 °C. The critical current for mitigating the microstructure deterioration of the deformed W foil was evaluated by changing the sample size. It is found that the optimal joining temperature is 1200 °C and the critical current density is below 418 A/cm^2. According to an optimized FAST joining process, the W foil laminate with a low microstructure deterioration and good interfacial bonding can be obtained. After analyzing these current profiles, it was evident that the high current density (sharp peak current) is the reason for the significant microstructure deterioration. An effective approach of using an artificial operation mode was proposed to avoid the sharp peak current. This study provides the fundamental knowledge of FAST principal parameters for producing advanced materials.

Keywords: tungsten foil laminate; field-assisted sintering technology; laminated toughening; critical electric current; operation mode

1. Introduction

Tungsten (W) possesses several advantages, including high melting-point, high density, high hardness, low thermal coefficient, low vapor pressure, good thermal/electrical conductivity and excellent chemical stability, which is widely applied in the fields of military industry, aerospace, electronics, nuclear energy [1]. However, the low-temperature brittleness of W materials due to the existence of unavoidable impurities is one of the bottleneck issues which strongly limit its application and processing [2]. In the past few decades, several approaches of adding alloying elements (rhenium) [3], adding second

phase nanoparticles [4], fiber toughening [5], laminated toughening [6] and plastic processing [7] have been carried out to address W brittleness. Among these toughening approaches, alloying and plastic processing obey the intrinsic toughening mechanism, which aims at improving the dislocation mobility and increasing the amount of mobile dislocation, respectively; the fiber toughening, laminated toughening, and addition of the second phase particles follow the extrinsic toughening mechanism, which can increase the fracture absorbing energy during fracture propagation [8].

Severely deformed W thin foil shows excellent ductility even at room temperature [9]. An advanced material concept of laminated composite using pure W foils has been proposed as an efficient solution for low-temperature brittleness, which combines both the toughening mechanisms of plastic processing and laminated toughening [10]. The laminated toughening can increase the fracture absorption energy due to the crack deflection. According to the different interface characteristics, the laminated toughening mechanisms can be classified into weak/strength (brittle) interface toughening [11] and plasticity interface toughening [12]. The validity of laminated toughening depends mainly on the interface strength [13]. In the past decade, numerous studies have focused on interfacial design by adding the interlayers of Ti [6,14], Ta [15], V [16], Cu [16,17], etc. For the W foil laminate, the component of severely deformed W foil features a poor microstructure stability due to the high density of defects [18]. This implies that recovery and recrystallization, i.e., microstructure deterioration, can occur during the joining process at a high temperature, which results in the brittleness of W foil. Therefore, the interface optimization and microstructure deterioration controlling are the main challenges for the production of the W foil laminate using a joining technique.

Due to the high melting point of W, in previous studies, the W foil laminate was always joined by diffusion bonding. Hot pressing (HP) with assisted pressure is one commonly used technique to join bulk W materials [17]. The pressure could ensure a good contact among W thin foils. Notably, joining of the W foil laminate using HP technique requires a high temperature, which would result in the microstructure deterioration of the W foil. Different from the HP technique, field-assisted sintering technology (FAST) is assisted additionally by an electrical current/field. It is widely used to join a variety of metal matrix materials [19], to consolidate the powder materials [20] and for heat treatment of the work-hardened metals [21]. It was reported that heat treatment for the deformed steel and AZ31 magnesium alloy in FAST apparatus can accelerate microstructure evolution but achieve a more uniform microstructure with a finer grain, compared with conventional heat treatment [21]. In the FAST system, the assisted current features the binary effects of Joule thermal and electro-migration [22]. The Joule thermal effect derives from the intrinsic electrical resistance of the sintering tools (e.g., graphite punches and die) and/or conductive green body. The electro-migration effect can accelerate atom diffusion [23] and defect annihilation [24]. This implies that the FAST joining process enhances diffusion bonding between adjoining W foils but may result in the ductility deterioration of the deformed W foils. Therefore, the profile of the electric current during the FAST joining process should be optimized.

The FAST process in the preparation of materials or components was intensively optimized by changing the temperature [25], heating rate [26], pressure [27], and sintering atmosphere [28]. However, rather little attention has been paid to the impact from the operation of the FAST apparatus. Generally, the operation mode of the FAST apparatus includes the automatic operation mode based on the designed temperature curves and the artificial operation mode according to a certain current profile. In addition, the selection of the temperature measurement methods during the FAST joining process is also different including K-type thermocouple (RT–1000 °C) and optical pyrometer (570–2000 °C). Different selection of the operation mode or temperature measurement method means different profiles of the electric current, which strongly impacts the interface bonding and microstructure evolution of W foil laminates.

In this work, a series of experiments of joining W foil laminate were carried out in a FAST apparatus. To balance the effective interfacial bonding and microstructure deterioration of the W foil laminate, the optimizations of joining temperature and electric current profile were performed. The joining temperature was optimized by changing temperature from 600 to 1400 °C with a temperature interval of 200 °C. The critical current for mitigating the microstructure deterioration of the deformed W foil was evaluated by changing the sample size following the same FAST joining process. Finally, an optimized joining process was used to fabricate the W foil laminate. According to these studies, the impact of the current profile due to the different operation mode or temperature measurement method on microstructure evolution of W foil laminate were evaluated.

2. Materials and Methods

2.1. Sample Preparation

The severely deformed W foils (purity 99.95%) fabricated by powder metallurgy and warm-rolling are supplied by XI'AN REFRA TUNGSTEN & MOLYBDENUM CO., LTD., Xi'An, China. The thickness of the W foils was approximately 100 μm. No heat treatment was performed after a warm-roll smoothing process. Figure 1 shows the production flow chart of the W foil laminate. The W foil wafers were cut from a W foil plate using electrical discharge machining (EDM). To remove the residual dirties during the EDM process, these W wafers were firstly cleaned in a boiling NaOH (8 wt.%) solution for 6–8 min, and then were processed with ultrasonic cleaning for 20 min in acetone and ethanol solution, respectively. Afterwards, these W wafers were dried under vacuum. Each sample of the W foil laminate in this study comprised 21 pieces of W wafer. Notably, the rolling direction (RD) of W wafers are along the same direction during the stacking process. Between the W wafers and the graphite tools, a molybdenum foil (~25 μm in thickness) and a graphite sheet (~0.2 mm) are used to prevent the carbon from graphite die to react with W wafers and for the convenience of demolding, respectively. The joining of the W foil laminate was carried out in a FAST apparatus (Labox-350, NJS Co., Ltd., Yokohama, Japan). During the FAST joining process, a pressure of 30 MPa was loaded on samples to ensure a good contact between adjacent W wafers. It should be pointed out that the temperature measuring position was 5 mm from the edge of the sample in the graphite die, as marked with the red dot in Figure 1. In addition, the temperature measurements using the K-type thermocouple or an optical pyrometer were calibrated before FAST joining.

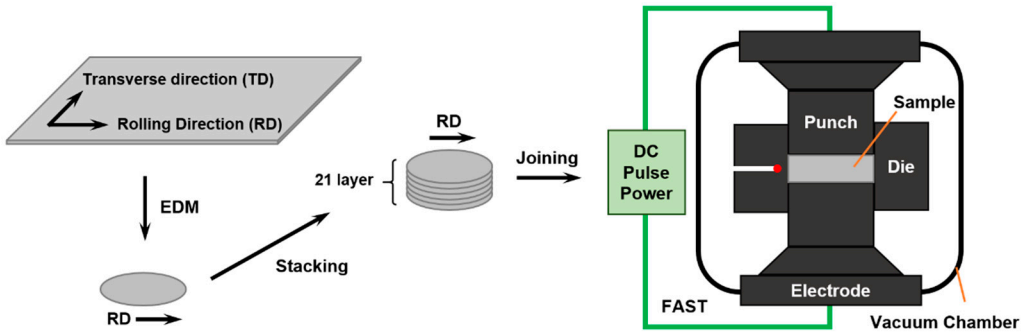

Figure 1. The process flow chart of the W foil laminates preparation.

In order to optimize the joining temperature, the W foil laminates with a diameter of Ø20 mm were FAST joined at a different temperature varied from 600 to 1400 °C in an automatic operation mode. The real-time temperature changes were monitored by an optical pyrometer. Figure 2a shows the real-time temperature change curves of the W foil laminates. The heating rate was 100 °C/min. After the samples were heated up to the designated temperature, they were cooled down in the furnace without holding time. Figure 2b shows the corresponding current density curves, which show a similar change

trend. Due to the detection limit of 570 °C for the optical pyrometer, there is a sharp peak current, almost reaching ~1300 A/cm^2.

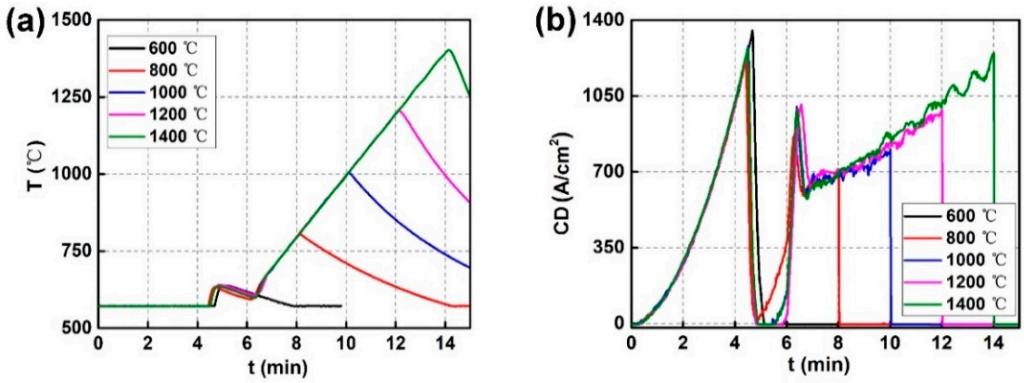

Figure 2. (**a**) The real-time temperature change curves and (**b**) the profiles of the current density (CD) change of the W foil laminates joined at different temperature.

To clarify the critical electric current for microstructure apparent deterioration, the samples of the W foil laminate with different diameters (Ø13, Ø20, and Ø25 mm) were FAST joined at 800 °C in an automatic heating mode. These three samples underwent the same FAST joining process with a heating rate of 100 °C/min, as shown in Figure 3a. Once these samples were heated up to 800 °C, they were cooled down by switching off the power. The temperature changes during the FAST joining process were measured by the K-type thermocouple. Figure 3b shows the current density change curves during the FAST joining process. Due to the different sample dimensions, the current density decreases with the increasing of the sample and presents a wave fluctuation. The maximum current density of Ø13, Ø20, and Ø25 mm samples fabrication are 630, 530, and 418 A/cm^2, respectively.

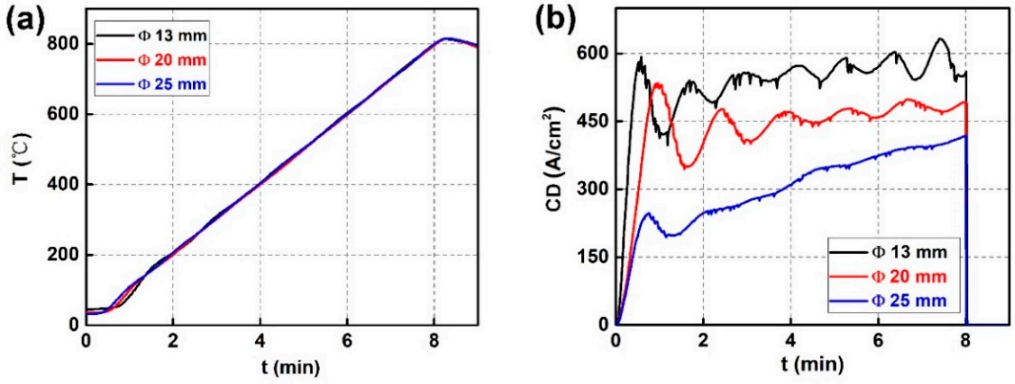

Figure 3. (**a**) FAST joining process and (**b**) the current density (CD) change curves of the W foil laminates with different diameters.

In addition, an optimized FAST joining process in an artificial operation mode was used to fabricate the W foil laminate with a diameter of Ø20 mm. Figure 4 shows the curves of current density and the corresponding temperature curve. The input current increased stepwise with a step rate of 100 A/min. When the current reached 1200 A (the responding current density is ~380 A/cm^2), the current value was held for 20 min. The final temperature reached ~1250 °C. During the FAST joining process, the temperature measurement was monitored by an optical pyrometer.

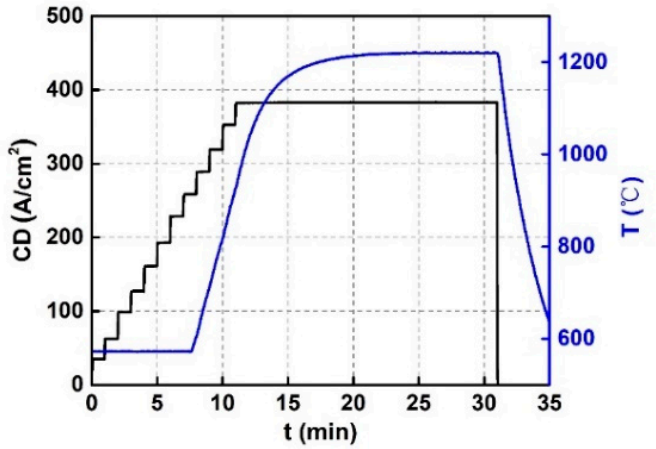

Figure 4. The change curves of current density (CD) and temperature during the FAST joining process of W foil laminate in an artificial operation mode.

2.2. Characterization

Metallographic microscopy (Axio Lab.A1, Sigma Zeiss, Jena, Germany) and field emission scanning electron microscopy (FESEM, Gemini 300, Sigma Zeiss, Jena, Germany) were used to characterize the microstructure before and after FAST joining process. For the microstructural characterization, the specimens were processed with grinding and mechanical polishing, followed by metallographic etching. During the etching process, the specimens were immersed in a boiling H_2O_2 solution for 2 min. Due to the defects (grain boundary and dislocation) being sensitive to the etchant [29], the metallographic structure was applied to assess qualitatively the changes in the defect density. Notably, the specimens were mounted with a conductive mosaic powders for the cross-section characterization.

The Vickers hardness measurement was used to evaluate the microstructure evolution of the W foil laminates after FAST joining at different temperature using a hardness detector (MH-3, Shanghai Everone Precision Instruments Co., Ltd., Shanghai, China). A load of 200 g was loaded on the polished cross section (RD-ND surface) for a duration of 10 s for each sample. To obtain reliable data, the Vickers hardness values were statistically calculated from 21 indentations, which measures from three W foil layers with 7 points for each layers. The thermal diffusivity (α) was also measured to indirectly reflect the interfacial bonding performance of the W foil laminates. This test was performed in a laser-flash system (LFA467, Netzsch, Selb, Germany) with an argon atmosphere and a temperature range from room temperature to 450 °C with a temperature interval of 50 °C. The specimen size for thermal diffusivity measurement was Ø12.7 mm in diameter and 2.0 mm in thickness. Notably, the direction of thermal diffusivity is the normal direction (ND) of the warm-rolled W wafer.

3. Results

3.1. Microstructure of the Original W Foil

To expediently evaluate the microstructure evolution, the microstructure of the original W foil was characterized. Figure 5a shows the metallographic structure of the W foil after etching. It shows the rolling surface (RD-TD), in which erosion traces are distributed. The high density of erosion traces means a high density of defects such as grain boundaries and dislocation. Figures 5b and 5c present the SEM images of the RD-TD surface and the RD-ND surface, respectively. The elongated rolling grain structure can be discovered. After measurement from Figure 5c, the size of the grain viewed from the transverse direction (TD) is up to tens of microns in RD and approximately 0.5 μm in ND.

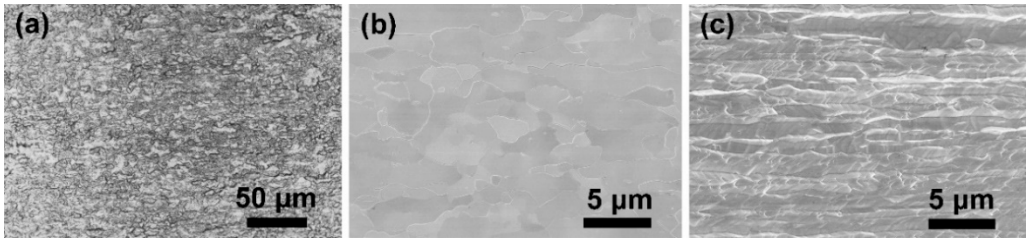

Figure 5. The microstructure of the original W foil. (**a**) Metallographic structure of the etched rolling surface, and SEM microstructure of (**b**) the rolling surface and (**c**) the side surface.

3.2. Joining Temperature Optimization

After FAST joining, the microstructure of the W foil laminates exhibits various degrees of recrystallization as a function of temperature change. Figure 6 shows the metallographic structures of the W foil laminates joined at different temperature, viewed from TD. In cases of FAST joining at 600 and 800 °C, as shown in Figure 6a,b, several large grains exist (as pointed with arrows). These imply that the recrystallization starts at 600 °C under the present FAST heating condition. If the joining temperature reaches 1000 °C (Figure 6c–e), it can be seen that the samples have completely recrystallized. Compared with the deformed W which underwent traditional heat treatment [30], in the FAST process, the recrystallization temperature was decreased, and the recrystallization process was accelerated. The enlarged SEM images focused on the interfaces of the W foil laminates were also presented in Figure 6. Significant gaps exist at the interfaces in cases of FAST joining at 600, 800, and 1000 °C, as shown in Figure 6(a_1), Figure 6(b_1) and the inserted image of Figure 6c, respectively. When the joining temperature reaches 1200 °C, it is hard to discover the obvious interface gap between W foils from the inserted images in Figure 6d,e. This indicates that the W foil laminates have a good interfacial bonding.

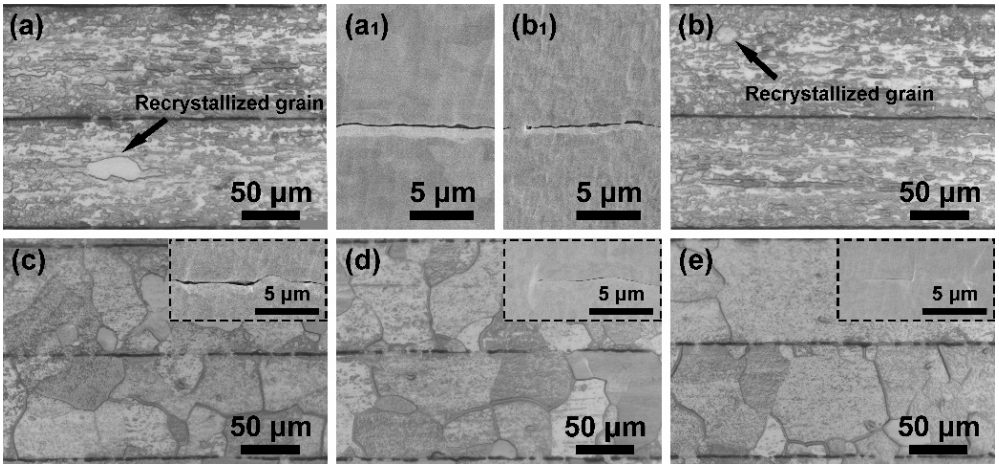

Figure 6. The metallographic structures viewed from transverse direction of the W foil laminates joined at different temperatures (**a**) 600 °C, (**b**) 800 °C, (**c**) 1000 °C, (**d**) 1200 °C, and (**e**) 1400 °C. (**a_1**,**b_1**) and the insert images are the SEM images of the corresponding interfaces.

Vickers hardness measurement was used to evaluate indirectly the microstructure evolutions of the deformed W materials during the annealing process [31]. Figure 7a shows the Vickers hardness of the W foil laminates after FAST joining at different temperatures. It shows a typical "S" type trend, which coincides well with the microstructure evolutions in Figure 6. The stepped descent occurs at 1000 °C, which is close to the recrystallization temperature of the W foil in case of FAST joining. Compared to the other cases, the hardness of the sample FAST joined at 1000 °C features a large error bar. This implies non-uniform microstructure due to the different degree of crystallization. Instead of the intrinsic and microscopic features, the thermal diffusivity is more sensitive to the macro-defects of a

pore or crack [32]. Therefore, it was used to evaluate the interfacial bonding performance of the W foil laminates after FAST joining at different temperatures. Figure 7b is the corresponding thermal diffusivity of the W foil laminates. Low thermal diffusivity exists in cases of the FAST joining at 600 and 800 °C, owing to the existence of interface gaps among W foils. Notably, the samples have a similarly high thermal diffusivity in the case of the FAST joining at 1200 and 1400 °C. This means that the W foil laminates joined at 1200 and 1400 °C have a similar interfacial bonding performance. Considering that the W foil laminate FAST joined at a high temperature would result in the microstructure deterioration to a different degree, the optimal FAST joining temperature is 1200 °C. When the sample joined at 1000 °C, the medium thermal diffusivity in Figure 7b would be related to the existence of some micro gaps at interface between W foils, as shown in Figure 6c.

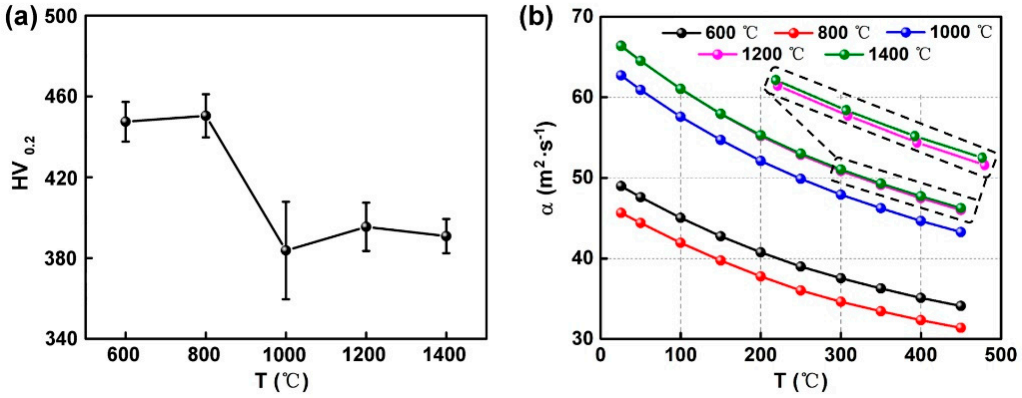

Figure 7. (**a**) The Vickers hardness and (**b**) the thermal diffusivity of the W foil laminates as a function of the joining temperature.

3.3. Current Density Optimization

From Figure 6, the microstructure of the W foil laminates shows an apparent deterioration when the FAST joining temperature reaches 1000 °C. For the convenience of clarifying the critical current density on microstructure evolution, the recrystallization due to the possible factor of temperature should be avoided. Therefore, the current density optimization of the W foil laminates was performed at 800 °C by changing sample's dimensions. Figure 8 shows the metallographic structure of the RD-TD surface of the W foil laminates. In contrast to the initial W foil in Figure 5a, the erosion trace decreases significantly with the decrease in sample size. Notably for the Ø13 mm sample (Figure 8a), the W foil laminate has fully recrystallized. The grain size experiences significant growth compared with the initial W foil in Figure 5b. This is due to the fact that to the Ø13 mm sample underwent the highest density of current. This verifies directly that the current could accelerate the microstructure evolution, which is mainly attributed to the electro-migration effect of the assisted current. In addition, the Ø25 mm sample underwent the lowest current density and exhibits the lightest changes in microstructure, as shown in Figure 8c. This means that the optimal current density for the FAST joining of W foil laminate is below 418 A/cm^2.

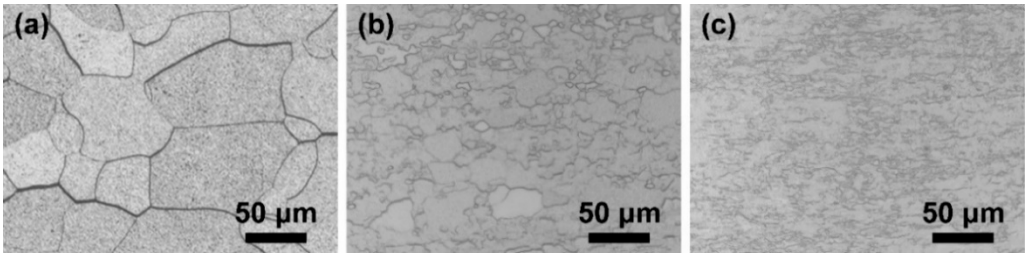

Figure 8. The metallographic structure of the W foil laminates with different diameter of (**a**) Ø13 mm; (**b**) Ø20 mm; (**c**) Ø25 mm after FAST joining at 800 °C.

3.4. FAST Joining Optimization

According to the above optimization of the joining temperature and current density, an optimized FAST joining process was explored. To control the temperature and current, the FAST apparatus was carried out in an artificial operation mode. Under the designed electric current loading mode, the maximum current density was 380 A/cm^2 and the corresponding joining temperature was ~1250 °C (Figure 4). Figure 9a is the metallographic structure viewed from TD of the W foil laminate. It still retains a large number of deformed grains, and only a few recrystallized grains exist. Compared with the samples FAST joined at 1000–1400 °C in an automatic operation mode (Figure 6c–e), the microstructure deterioration of the W foil laminates was mitigated. Figure 9b shows a magnified interface structure of the sample characterized by SEM. It has a similar interface structure with the samples in Figure 6d,e, in that no obvious gap exists at the interface. Therefore, carrying out the FAST joining in an artificial operation mode, the microstructures deterioration of the W foil laminate can be inhibited while ensuring good interfacial bonding.

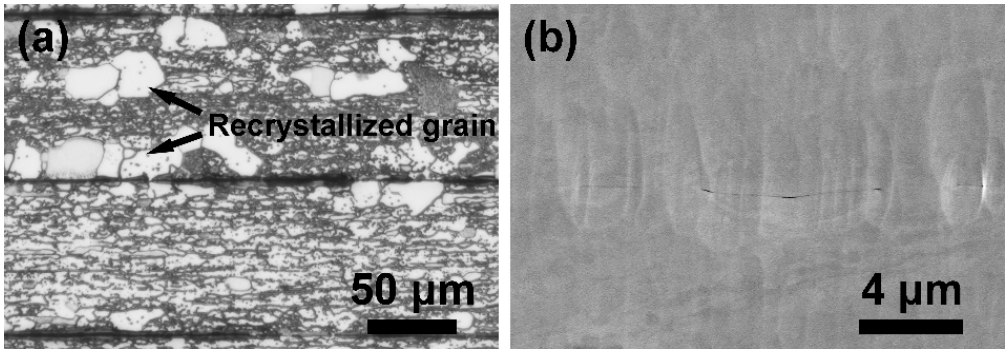

Figure 9. (**a**) The metallographic structure and (**b**) a representative W–W interface of the W foil laminate FAST joined in an artificial operation mode.

4. Discussion

From the aforementioned results in Figures 6, 8 and 9, two phenomena of microstructure evolution deserve attention. One is that only a few recrystallized grains were discovered for the sample in Figure 6b, but a fully recrystallized microstructure occurred for the sample in Figure 8a, although both of them were joined at the same temperature (800 °C). The other is that a fully recrystallized microstructure existed in the sample after FAST joining at 1000 °C (Figure 6c), but did not present in the sample joined at 1250 °C (Figure 9a). Essentially, the microstructure evolution (recovery, recrystallization and grain growth) of the severely deformed W foils is the process of mass diffusion. The activation energy for mass diffusion normally depends largely on the temperature [33]. However, according to this study, it seems that the decisive factor for the microstructure evolution during the FAST joining process is not the temperature (i.e., thermal effect), but rather the assisted current induced the non-thermal effect. Therefore, the microstructure evolution will be revealed based on the electric current profiles in the following discussion.

4.1. FAST Operation Conditions

Because the automatic operation mode is based on the designed temperature curves, the corresponding current profile is sensitive to the temperature measurement method. In Figures 2 and 3, the two cases were FAST joined in an automatic operation mode, but with different temperature measurement methods. In the cases of the W foil laminate joined at 600–1400 °C, the temperature measurement was monitored by an optical pyrometer. Within the lower limit (570 °C) of the optical pyrometer, the FAST apparatus loses the reference temperature for heating. Therefore, the electric current profile shows a sharp peak with a current density up to ~1300 A/cm^2, as presented in Figure 2. If the temperature change was measured by a K-type thermocouple in case of the W foil laminate FAST joined at 800 °C

(Figure 3), the electric current profiles show a smooth increase with the temperature rise. It can be concluded that the existence of a sharp peak current during the W foil laminates FAST joined in an automatic operation mode does not depend on the joining temperature, but relies on the temperature measurement method.

In the artificial operation mode, the heating process is performed according to the established current curve. This means that changing the temperature measurement method has no effect on the current curve. The selection of the temperature measurement method merely depends on the temperature scope of FAST joining. In the case of the FAST joining in an artificial operation mode (Figure 4), the current profiles can be precisely controlled avoiding the sharp peak current.

4.2. Critical Electric Current

As similar as the deformed metals or alloys that have a recrystallization temperature are, the severely deformed W foil would have a critical electrical current for the apparent microstructure evolution during the FAST joining process. The experiment in Figure 3 aims at roughly evaluating the critical electric current. Based on the results in Figure 8, when the electric current density is below 418 A/cm^2, the microstructure deterioration of W foil can be avoided. The microstructure of the Ø13 mm sample fully recrystallized (Figure 8a) when undergoing a high current density of >600 A/cm^2. From the current profiles in Figure 2, the very high current density above 600 A/cm^2 could be the reason for the formation of the few recrystallized grains in the case of FAST joining at 600 °C (Figure 6a) and 800 °C (Figure 6b). Due to the applied current with a high density during the FAST joining process, the samples have a full recrystallized microstructure, as shown in Figure 6c–e.

From the current profiles in Figures 2 and 3, the sample in Figure 6b withstands a sharp peak current with a shorter duration time, while the sample in Figure 8a withstands a sustained high-density current for a longer time. Although these two samples were FAST joined at a similar temperature of 800 °C, the sample of Figure 8a exhibits apparent microstructure deterioration. Since the microstructure evolution is a mass diffusion process, the current action time plays a critical role in the significant recrystallization microstructure in additional to the critical electrical current.

On the other hand, from the corresponding current profile in Figure 4, the maximum current density is ~380 A/cm^2, which is below the critical current of the apparent microstructure evolution. The microstructure of the W foil laminate only features a few recrystallized grains (Figure 9a), although after FAST joining at a high temperature of 1250 °C, maintained for 20 min. In the case of the sample FAST joined at 1000 °C, the current profile shows that the current density is far larger than ~380 A/cm^2, as shown in Figure 2. Although the duration time of the high current density is short, the sample exhibits a fully recrystallized microstructure (Figure 6c). Therefore, this indicates that the current action time has no obvious effect on the microstructure deterioration in cases of the current being below the critical value.

5. Summary and Outlook

When producing the W foil laminate in a FAST apparatus, the main challenge is to balance the influence of assisted current on microstructure deterioration and interfacial bonding. It can be solved to a certain extent by using an artificial operation mode. According to this work, the critical electrical current for avoiding an apparent microstructure deterioration is below 418 A/cm^2 and the optimal joining temperature for a good interfacial bonding is 1200 °C. In the case of the W foil laminate loaded with a maximum current density of 380 A/cm^2 for 20 min (the corresponding temperature is 1250 °C), a low microstructure deterioration and good interfacial bonding can be obtained.

The possible influence factors (joining temperature, critical electric current and current action time) on microstructure evolution of the W foil laminate were discussed from the perspectives of the FAST operation mode and temperature measurement method. If the

temperature measurement is based on the optical pyrometer, the current profile exhibits a sharp peak current, which accelerates the microstructure deterioration. In this case, the current action time plays a critical role in significant recrystallization in additional to the critical electrical current. If the FAST joining is carried out in an artificial operation mode, the current profile can be effective controlled. The current action time has no obvious effect on the microstructure deterioration in case of the input current below the critical current.

In the case of the sample joined at 600 °C (Figure 6a) in an automatic operation mode, the local recrystallization may be related to the sharp peak current. Generally, the preferential recrystallization behavior in traditional heat treatment is due to the locally high density of defects [34]. However, it is hard to establish the relationship between the local recrystallization and the locally high density of defects because the defects are the obstacles to current flow. This suggests the need for an in-depth study to clarify the formation mechanism of the local recrystallization.

In addition, the critical roles of current density and current action time on microstructure evolution has been discussed in this work. Notably, the current density and current action time in fact have both synergistic and competitive effects on microstructure evolution. Therefore, further study is required to investigate whether the microstructure involution depends on current density or current action time.

Author Contributions: X.T. performed conceptualization, writing—original draft, methodology, investigation, formal analysis. W.W. and X.C. performed investigation, visualization. J.L., L.L. performed investigation, resources. Y.M., A.L., F.K., P.B., J.W.C. and C.L. performed review and editing. Y.W. performed conceptualization and project administration. All authors have read and agreed to the published version of the manuscript.

Funding: This work was funded by the National Natural Science Foundation of China (Grant No. 52020105014, 52001104), the Fundamental Research Funds for the Central Universities (Grant No. JZ2019HGTA0040, JZ2019HGBZ0113, PA2019GDZC0096, JZ2020HGQB0230), the Natural Science Foundation of Anhui Province (Grant No. 201904b11020034, 1908085ME115), the High Education Discipline Innovation Project "New materials and Technology for Clean Energy" (B18018) and the International Postdoctoral Exchange Fellowship Program of Helmholtz-OCPC (No. ZD20191015).

Data Availability Statement: Data are contained within the article.

Conflicts of Interest: The authors declare no conflict of interest.

References

1. Huang, L.; Jiang, L.; Topping, T.D.; Dai, C.; Wang, X.; Carpenter, R.; Haines, C.; Schoenung, J.M. In situ oxide dispersion strengthened tungsten alloys with high compressive strength and high strain-to-failure. *Acta Mater.* **2017**, *122*, 19–31. [CrossRef]
2. Butler, B.G.; Paramore, J.D.; Ligda, J.P.; Ren, C.; Fang, Z.Z.; Middlemas, S.C.; Hemker, K.J. Mechanisms of deformation and ductility in tungsten—A review. *Int. J. Refract. Met. Hard Mater.* **2018**, *75*, 248–261. [CrossRef]
3. Yoshida, N. Review of recent works in development and evaluation of high-Z plasma facing materials. *J. Nucl. Mater.* **1999**, *266–269*, 197–206. [CrossRef]
4. Tan, X.Y.; Li, P.; Luo, L.M.; Xu, Q.; Tokunaga, K.; Zan, X.; Wu, Y.C. Effect of second-phase particles on the properties of W-based materials under high-heat loading. *Nucl. Mater. Energy* **2016**, *9*, 399–404. [CrossRef]
5. Mao, Y.; Coenen, J.W.; Riesch, J.; Sistla, S.; Almanstötter, J.; Reiser, J.; Terra, A.; Chen, C.; Wu, Y.; Raumann, L.; et al. Fracture behavior of random distributed short tungsten fiber-reinforced tungsten composite. *Nucl. Fusion* **2019**, *58*, 086034. [CrossRef]
6. Chen, C.; Qian, S.F.; Liu, R.; Wang, S.; Liao, B.; Zhong, Z.H.; Cao, L.F.; Coenen, J.W.; Wu, Y.C. The microstructure and tensile properties of W/Ti multilayer composites prepared by spark plasma sintering. *J. Alloys Compd.* **2019**, *780*, 116–130. [CrossRef]
7. Zhang, X.X.; Yan, Q.Z.; Yang, C.T.; Wang, T.N.; Ge, C.C. Microstructure, mechanical properties and bonding characteristic of deformed tungsten. *Int. J. Refract. Met. Hard Mater.* **2014**, *43*, 302–308. [CrossRef]
8. Wu, Y.C. The routes and mechanism of plasma facing tungsten materials to improve ductility. *Acta Metall. Sin.* **2019**, *55*, 171–180.
9. Vladica, N.; Stefan, W.; Daniel, F.; Reinhard, P. Fracture toughness evaluation of UFG tungsten foil. *Int. J. Refract. Met. Hard Mater.* **2018**, *76*, 214–225.
10. Ritchie, R.O. The conflicts between strength and toughness. *Nat. Mater.* **2011**, *10*, 817–822. [CrossRef]
11. Bermejo, R.; Danzer, R. High failure resistance layered ceramics using crack bifurcation and interface delamination as reinforcement mechanisms. *Eng. Fract. Mech.* **2010**, *77*, 2126–2135. [CrossRef]
12. Bloyer, D.R.; Ritchie, R.O.; Venkateswara, R. Fracture toughness and R-curve behavior of laminated brittle-matrix composites. *Metall. Mater. Trans. A* **1998**, *29*, 2483–2496. [CrossRef]

13. Liu, J.Q.; Chen, X.; Tan, X.Y.; Wang, W.J.; Wu, M.; Luo, L.M.; Zhu, X.Y.; Wu, Y.C. Toughening mechanism and research status of tungsten layered materials. *Chin. J. Nonferrous Met.* **2020**, *30*, 2331–2339.
14. Reiser, J.; Franke, P.; Weingäertner, T.; Hoffmann, J.; Hoffmann, A.; Rieth, M. Tungsten laminates made of ultrafine-grained (UFG) tungsten foil—Ageing of tungsten-titanium (W-Ti) laminates. *Int. J. Refract. Met. Hard Mater.* **2015**, *51*, 264–274. [CrossRef]
15. Yan, Z.; Xu, G.; Suo, J. Effect of transition layer on properties of Tungsten-Tantalum (W-Ta) laminated composite. *Metals* **2020**, *10*, 588. [CrossRef]
16. Nogami, S.; Hazama, T.; Noto, H.; Nagasaka, T.; Hasegawa, A. Laminated composites using potassium doped tungsten. *Fusion Eng. Des.* **2020**, *161*, 111894. [CrossRef]
17. Reiser, J.; Garrison, L.; Greuner, H.; Hoffmann, J.; Weingärtner, T.; Jäntsch, U.; Klimenkov, M.; Franke, P.; Bonk, S.; Bonnekoh, C.; et al. Ductilisation of tungsten (W): Tungsten laminated composites. *Int. J. Refract. Met. Hard Mater.* **2017**, *69*, 66–109. [CrossRef]
18. Reiser, J.; Rieth, M.; Dafferner, B.; Hoffmann, A.; Yi, X.O.; Armstrong, D.E.J. Tungsten foil laminate for structural divertor applications—Analyses and characterisation of tungsten foil. *J. Nucl. Mater.* **2012**, *424*, 197–203. [CrossRef]
19. Galatanu, A.; Galatanu, M.; Enculescu, M.; Reiser, J.; Sickinger, S. Thermophysical and mechanical properties of W-Cu laminates produced by FAST joining. *Fusion Eng. Des.* **2019**, *146*, 2371–2374. [CrossRef]
20. Wu, Y.C. Manufacturing of tungsten and tungsten composite for fusion application via different routes. *Tungsten* **2019**, *1*, 80–90. [CrossRef]
21. Park, J.W.; Jeong, H.J.; Jin, S.W.; Kim, M.J.; Lee, K.; Kim, J.J.; Hong, S.T.; Han, H.N. Effect of electric current on recrystallization kinetics in interstitial free steel and AZ31 magnesium alloy. *Mater. Character.* **2017**, *133*, 70–76. [CrossRef]
22. Deng, S.H.; Yuan, T.C.; Li, R.D.; Zhang, M.; Xie, S.Y.; Wang, M.B.; Li, L.B.; Yuan, J.W.; Weng, Q.G. Influence of electric current on interdiffusion kinetics of W-Ti system during spark plasma sintering. *Int. J. Refract. Met. Hard Mater.* **2018**, *75*, 184–190. [CrossRef]
23. Deng, S.H.; Li, R.D.; Yuan, T.C.; Xie, S.Y.; Zhang, M.; Zhou, K.C.; Cao, P. Direct current enhanced densification kinetics during spark plasma sintering of tungsten powder. *Scr. Mater.* **2018**, *143*, 25–29. [CrossRef]
24. Liang, C.L.; Lin, K.L. The microstructure and property variations of metals induced by electric current treatment: A review. *Mater. Charact.* **2018**, *145*, 545–555. [CrossRef]
25. Zhou, Y.F.; Zhao, Z.Y.; Tan, X.Y.; Luo, L.M.; Xu, X.; Zan, X.; Xu, Q.; Tokunaga, K.; Zhu, X.Y.; Wu, Y.C. Densification and microstructure evolution of W-TiC-Y_2O_3 during spark plasma sintering. *Int. J. Refract. Met. Hard Mater.* **2019**, *79*, 95–101. [CrossRef]
26. Wang, W.J.; Tan, X.Y.; Liu, J.Q.; Chen, X.; Wu, M.; Luo, L.M.; Zhu, X.Y.; Chen, H.Y.; Mao, Y.R.; Litnovsky, A.; et al. The influence of heating rate on W-Cr-Zr alloy densification process and microstructure evolution during spark plasma sintering. *Powder Technol.* **2019**, *370*, 9–18. [CrossRef]
27. Yang, S.P.; Wang, W.J.; Tan, X.Y.; Zhu, H.J.; Litnovsky, A.; Klein, F.; Mao, Y.R.; Coenen, J.W.; Linsmeier, C.; Luo, L.M.; et al. Influence of the applied pressure on the microstructure evolution of W-Cr-Y-Zr alloys during the FAST process. *Fusion Eng. Des.* **2021**. [CrossRef]
28. Hu, Z.Y.; Zhang, Z.H.; Cheng, X.W.; Wang, F.C.; Zhang, Y.F.; Li, S.L. A review of multi-physical fields induced phenomena and effects in spark plasma sintering: Fundamentals and applications. *Mater. Des.* **2020**, *191*, 108662.
29. Cho, K.S.; Sim, H.S.; Kim, J.H.; Choi, J.H.; Lee, K.B.; Yang, H.R.; Kwon, H. A novel etchant for revealing the prior austenite grain boundaries and matrix information in high alloy steels. *Mater. Charact.* **2008**, *59*, 786–793. [CrossRef]
30. Umberto, M.C.; Angela, T.; Chloé, D.; Wolfgang, P. Recovery and recrystallization kinetics of differently rolled, thin tungsten plates in the temperature range from 1325 °C to 1400 °C. *Nucl. Mater. Energy* **2019**, *20*, 100701.
31. Umberto, M.C.; Wolfgang, P. Stagnant recrystallization in warm-rolled tungsten in the temperature range from 1150 °C to 1300 °C. *Fusion Eng. Des.* **2019**, *146*, 814–817.
32. Vincent, C.; Silvain, J.F.; Heintz, J.M.; Chandra, N. Effect of porosity on the thermal conductivity of copper processed by powder metallurgy. *J. Phys. Chem. Solids* **2012**, *73*, 499–504. [CrossRef]
33. Rollett, A.; Humphreys, F.; Rohrer, G.S.; Hatherly, M. *Recrystallization and Related Annealing Phenomena*, 2nd ed.; Pergamon: Oxford, UK, 2004.
34. Alaneme, K.K.; Okotete, E.A. Recrystallization mechanisms and microstructure development in emerging metallic materials: A review. *J. Sci. Adv. Mater. Dev.* **2009**, *4*, 19–33. [CrossRef]